PHYSICAL REVIEW E **106**, 054702 (2022)

Comparative dielectric and thermally stimulated-depolarization-current studies of the liquid crystal dimers 1″,9″-bis(4-cyanobiphenyl-4′-yl) nonane and heptane and a binary mixture between them, close to the glass transition

Jordi Sellarès,[1] José Antonio Diego,[1] David O. López,[2] Josep Salud,[2] Beatriz Robles-Hernández,[3,4]
María Rosario de la Fuente,[4] Juan Carlos Cañadas,[1] Miguel Mudarra,[1] Victor López de Rioja,[2]
Rafael Levit,[5] and Sergio Diez-Berart[2,*]
[1]*DILAB, Departament de Física, E.S.E.I.A.A.T. Universitat Politècnica de Catalunya, Colom 11, 08222 Terrassa, Spain*
[2]*Grup de les Propietas Físiques del Materials (GRPFM), Departament de Física, E.T.S.E.I.B. Universitat Politècnica de Catalunya, Avinguda Diagonal, 647, 08028 Barcelona, Spain*
[3]*Donostia International Physics Center, Manuel Lardizabal Ibilbidea 4, 20018 Donostia, Spain*
[4]*Departamento de Física Aplicada II, Facultad de Ciencia y Tecnología, Universidad del País Vasco, Apartado 644, E-48080 Bilbao, Spain*
[5]*Caracterització Elèctrica dels Materials i Dispositius (CEMAD), Departament de Física, E.T.S.E.I.B. Universitat Politècnica de Catalunya, Avinguda Diagonal, 647, 08028 Barcelona, Spain*

(Received 15 September 2022; revised 7 October 2022; accepted 27 October 2022; published 21 November 2022)

We have performed dielectric spectroscopy and thermally stimulated-depolarization-current experiments to study the molecular dynamics of the twist-bend nematic phase close to the glass transition of two members of the 1″,7′-bis(4-cyanobiphenyl-4′-yl)alkane homologous series (CB*n*CB): the liquid crystal (LC) dimers CB9CB and CB7CB, as well as a binary mixture of both. By doping CB9CB with a small quantity of CB7CB, the crystallization is inhibited when cooling the sample down, while the bulk properties of CB9CB are retained and we can investigate the supercooled behavior close to the glass transition. The study reveals that the inter- and intramolecular interactions of the mixture are similar to those of pure CB9CB and confirms that there is a single glass transition in symmetric LC dimers.

DOI: 10.1103/PhysRevE.106.054702

I. INTRODUCTION

Liquid crystal (LC) dimers are compounds formed by two rigid moieties, linked by a flexible spacer [1,2]. Even though LC dimers were reported by Vorländer almost one century ago [3], it was not until the works by Griffin and Britt in the early 1980's that they attracted the interest of the liquid crystal community [4,5]. In these works, LC dimers were shown to be the fundamental units of semiflexible LC polymers, in order to facilitate the study of these high molecular weight compounds [4,5]. With time, research on LC dimers has become more and more important within the field of liquid crystals, as their chemical and physical properties make them optimal candidates for many technological applications [1,2,5–23]. In the present work, we are specifically interested in three specific properties of LC dimers: (1) the ability of bent achiral molecules to form chiral structures, in particular, the twist-bend nematic (N_{TB}) phase, which has been the subject of intense research effort during the last decade [15,19,23–37]; (2) the interesting molecular dynamics of these compounds, as the flexible spacer introduces a coupling between the rigid cores that induces the existence of additional dielectric relaxation modes, in comparison to LC monomers [9,13,15,30,33,37–42]; (3) the glassy behavior of the mentioned dielectric relaxation modes in mesophases that can be supercooled and, ultimately, vitrified [8,18,21,23,43,44].

The N_{TB} mesophase was predicted by Meyer [24] and Dozov [25]. In such a phase, achiral molecules with intrinsic curvature (bent-shaped molecules) arrange in a chiral helicoidal structure, with the nematic director exhibiting periodic bend and twist deformations. This has been an absolute hot topic in the LC community for more than a decade now since it was experimentally discovered in the LC dimer 1″,7′-bis(4-cyanobiphenyl-4′-yl)heptane (CB7CB) by some of the authors of this work, among others [15], and it remains an open field of research. Furthermore, there still is some controversy and extensive debate concerning the design of materials exhibiting the N_{TB} mesophase, as well as its structure and properties [20,22,45].

Mesogenic molecules have polar groups and, therefore, molecular dynamics can be analyzed by dielectric spectroscopy measurements. Taking the Nordio-Rigatti-Segre theory for calamitic LC [46] as a basis, together with some experimental results [13], Stocchero *et al.* [9] developed a theory for the dielectric relaxation of LC dimers, that has been proven valid several times [33,37–42]. They predicted that a symmetric LC dimer (where both rigid moieties are the same ones) would exhibit two dielectric relaxation modes in the nematic phase: the low-frequency one due to coupled flip-flop reorientations of the rigid units (mode m_1) and the one at high-frequency due to a mixed mechanism of reorientations of the rigid units around their long axes and of precessions

---

[*] sergio.diez@upc.edu

around the molecular director of the mesophase (mode m_2). When the rigid units are not equal (nonsymmetric LC dimer), the high-frequency mode, m_2, remains unaltered, but there are two low-frequency modes, corresponding to flip-flop reorientations of both rigid units: one at lower frequencies (m_{1L}) and the other one at intermediate frequencies (m_{1H}). These relaxation modes of LC dimers are transmitted from the nematic phase, through the phase transition, to the smectic-*A* phase [40,42–44] and, also, to the twist-bend nematic phase, when present [15,18,30,33,37,42].

Molecular (and intramolecular) reorientations are the consequence of an existing molecular dynamic disorder. These reorientations are possible as long as molecules (or their reorienting parts) have enough “free” volume at their disposal and they appear in fluid phases, such as the isotropic, liquid crystalline mesophases, or orientationally disordered ones. In some cases, when a compound in a phase showing molecular dynamic disorder is cooled down fast enough, the phase can be supercooled and, ultimately, vitrified at the so-called glass transition temperature, T_g [47–52]. As the compound is cooled down, the “free” volume of the molecules gets smaller and, at the glass transition, the reorientations are hindered, their relaxation time being quite long. This means that the molecular dynamic disorder is frozen. It may be the case when several different molecular reorientations are present in a fluid phase, that not all of them are frozen at the glass transition [53–55] and that two different molecular reorientations lead to two different glass transition temperatures [21,43,44]. This last result has been found in some nonsymmetric LC dimers, where the glass transition with the lowest temperature is due to the freezing of the reorientations of the smaller rigid moieties and the highest temperature one is due to the freezing of the reorientations of the bulkier rigid ones. At the glass transition temperature, the heat capacity of the compound shows a jump, as some disorder that does not contribute to the heat capacity below T_g gets activated at this temperature. Therefore, calorimetric measurements allow the determination of T_g. Also, as the molecular dynamics becomes frozen, the glass transition temperature can be determined by dielectric spectroscopy, with the convention that the relaxation time of the “frozen” reorientations at T_g is ∼100 s. A third and very powerful technique in studying the glass transition is thermally stimulated-depolarization currents (TSDCs), with which a usually complex dielectric relaxation mode can be separated into its several elementary contributions. TSDCs are somewhat equivalent to dielectric spectroscopy measurements at very low frequencies (<1 mHz) [56]. They are, therefore, complementary techniques. According to Stocchero’s theory [9] and some experimental results, it seems that for symmetric LC dimers just one glass transition temperature should be present. Nevertheless, TSDC measurements are the most suitable to confirm this assumption.

The glassy behavior study through dielectric spectroscopy has already been performed in CB7CB [18]. Other LC dimers exhibiting the N_{TB} phase do not vitrify at accessible cooling rates to develop a dielectric analysis [30,33]. Specifically, CB9CB crystallizes about 80 K above T_g, if it is not cooled down fast enough [33]. One way to overcome crystallization and allow the glassy behavior study is by doping the material with nanoparticles [21]. Another possibility is to prepare binary mixtures of compatible compounds, one of them showing a glass transition when cooling at slow rates. We have recently shown, by calorimetric experiments, how some binary mixtures CB9CB + CB7CB, with different relative concentrations of both pure compounds, vitrify at slow cooling rates [57], which allows the present study of the molecular dynamics of these mixtures close to the glass transition. Static dielectric properties and elastic constants of one of such mixtures (0.46 mole fraction of CB9CB) have also been studied, yet far from the glass transition [42].

The first goal of the present work is to study the molecular dynamics close to the glass transition of a CB9CB-like compound by dielectric spectroscopy. For this purpose, we have prepared a binary mixture of CB9CB with a small quantity of CB7CB. The second goal is the analysis of this mixture as well as of the pure compounds, CB9CB and CB7CB, by TSDC measurements. The N_{TB} glassy state is experimentally studied, and with the help of the TSDC technique, we will confirm if there is just one glass transition temperature.

The paper is organized as follows: We start presenting the experimental methods before exposing and analyzing the results of both dielectric spectroscopy and TSDC measurements and, finally, we summarize the main conclusions of the work.

II. EXPERIMENTAL SECTION

A. Materials

Three different compounds were measured: CB7CB, CB9CB, and a binary mixture of 0.96 mole fraction of CB9CB. Pure CB9CB and CB7CB liquid crystal dimers were synthesized and purified according to the methodology reported in the work by Barnes *et al.* [58]. The binary mixture was prepared in sealed aluminum pans and heated to the isotropic phase in an ultrasonic bath [36].

B. Methods

Modulated differential scanning calorimetry (MDSC) measurements were made for a standard study of the overall thermal behavior of the mixture. Measurements were made on heating, at 1 K min^{-1}, from room temperature up to the isotropic phase. Modulation parameters (temperature amplitude and oscillation period) were ±0.5 K and 60 s. A sample mass of ∼3 mg was selected to ensure a uniform thin layer within the aluminum pans.

Measurements of the complex dielectric permittivity were performed with an Alpha impedance analyzer from Novocontrol, the frequencies ranging from 10^{-3} to 10^{6} Hz. The cell consists of two gold-plated brass electrodes (diameter 5 mm) separated by silica spacers, making a plane capacitor about 50 μm thick. The sample is held in a cryostat, and the temperature is controlled via a System Quatro from Novocontrol. Additional details of the experimental technique can be found elsewhere [54,59]. Dielectric measurements were performed on cooling with stabilization at different temperature steps and temperature control on the order of 20 mK.

Thermally stimulated-depolarization-current (TSDC) experiments were performed on commercial Linkam cells filled with liquid crystals by capillarity. The inner side of the cell had 1 cm^2 indium tin oxide (ITO) coated electrodes at a

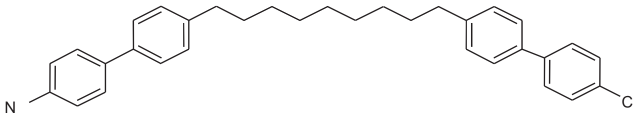

Scheme 1: CB9CB molecule.

distance of 5 μm. These cells were placed in a custom-built experimental setup where the temperature was controlled with a Eurotherm 904P temperature controller and registered with an accuracy of 0.1 K using a PT-100 thermoresistance thermometer located near the sample. A Heinzinger LNC 6000 voltage source was used to apply an electric field of 2.4 kV/mm to the samples. The depolarization currents were recorded using a Keithley 6512 electrometer.

III. RESULTS AND DISCUSSION

The liquid crystal dimers CB7CB and CB9CB consist of two cyanobiphenyl groups attached by a flexible alkyl chain with seven and nine carbons, respectively, as shown in Schemes 1 and 2.

The dielectric behavior of CB7CB, both far from the glass transition and close to it, has already been published [15,18]. Concerning CB9CB, the dielectric study has been made far from the glass transition, as the compound crystallizes ~80 K above T_g [33]. In order to avoid crystallization, binary mixtures of CB9CB with CB7CB, with different proportions of each pure compound, have been prepared. A preliminary thermal analysis of some mixtures has been reported [57]. They show the N_{TB} mesophase, which can be supercooled and vitrified ($[N_{\mathrm{TB}}]_{\mathrm{gl}}$) at slow cooling rates ($\leqslant 1$ K/min). For the present work, we have selected the binary mixture 0.96 mole fraction of CB9CB, as it is the closest to pure CB9CB we have been able to get in which the N_{TB} mesophase vitrifies at slow cooling rates. The analyzed mixture can be considered as CB9CB doped with a very small quantity of CB7CB, being an optimum candidate to study the dielectric behavior of a CB9CB-like material close to the glass transition. The phase sequence of the mixture, measured by MDSC on heating, is [57]

$$[N_{\mathrm{TB}}]_{\mathrm{gl}} - 277.4\,\mathrm{K} - \mathrm{Cry} - 351.1\,\mathrm{K} - N_{\mathrm{TB}} \\ - 378.1\,\mathrm{K} - N - 394.2\,\mathrm{K} - I.$$

After the glass transition, when the sample is heated from $[N_{\mathrm{TB}}]_{\mathrm{gl}}$, there is an irreversible crystallization, showing a typical phase sequence on heating, similar to that of pure CB9CB [33].

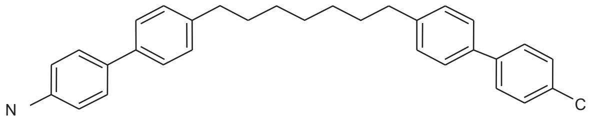

Scheme 2: CB7CB molecule.

A. Dielectric spectroscopy

We begin the discussion of the results with those from dielectric spectroscopy measurements of the mixture and the comparison with the published results of pure CB7CB [15,18] and CB9CB [33]. As the aim of the present work is to focus on the glassy behavior of the compounds, we have just performed these measurements, for the mixture, in the frequency range from 1 mHz to 1 MHz.

Figure 1 shows the real (filled circles) and imaginary (empty circles) parts of the complex dielectric permittivity in the supercooled twist-bend nematic phase at 303 K [Fig. 1(a)], 293 K [Fig. 1(b)], and 283 K [Fig. 1(c)] for the mixture with a dc bias of 35 V, the sample being homeotropically aligned. The values of the imaginary part are represented in a $\log_{10}$ scale. It must be noted that, as long as the sample approaches the glass transition temperature, the high conductivity hides the low-frequency mode if no bias is applied and it cannot be analyzed. The mixture seems to have some amount of crystallized material that induces a high conductivity. This fact will be later confirmed when analyzing the TSDC results.

Solid lines in Fig. 1 correspond to the fittings of experimental data to the empirical function:

$$\varepsilon(\omega) = \sum_k \frac{\Delta\varepsilon_k}{[1+(i\omega\tau_k)^{\alpha_k}]^{\beta_k}} + \varepsilon_\infty - i\frac{\sigma_{\mathrm{dc}}}{\omega\varepsilon_0}, \qquad (1)$$

where k accounts for all the relaxation modes in the N_{TB} mesophase, and each one is fitted according to the Havriliak-Negami function; $\Delta\varepsilon_k$ is the dielectric strength of the k relaxation mode and τ_k is its characteristic relaxation time, related to the frequency of maximum dielectric loss; α_k and β_k are parameters that describe the shape (width and symmetry, respectively) of the relaxation spectra; ε_∞ is the dielectric permittivity at high frequencies (yet lower than those corresponding to resonance phenomena) and σ_{dc} is the electric conductivity. The shape parameters (α and β) are a measure of the distributed nature of the relaxation mode. When they both, α and β, are equal to 1, we obtain a simple nondistributed Debye relaxation mode.

As shown in Fig. 1, there are two relaxation modes at temperatures far enough from the glass transition (such as 303 and 293 K), as happens for the pure compounds CB7CB [15,18] and CB9CB [33]. According to Stocchero's model [9], the low-frequency mode m_1 is associated with the flip-flop motion of the cyanobiphenyl group, and the high-frequency mode m_2 is due to reorientations of the cyanobiphenyl groups around their long axes and precessions of such rigid units around the nematic director. The low-frequency mode m_1 is Debye-like ($\alpha = \beta = 1$), while the high-frequency mode m_2, is Cole-Cole ($\alpha = 0.6$ and $\beta = 1$). In pure CB7CB and CB9CB, the low-frequency modes are both Debye-like, whereas the high-frequency ones are Cole-Cole, with $\alpha = 0.7$ and 0.8 for CB7CB and CB9CB, respectively [18,33]. When approaching the glass transition, both relaxation modes converge into one single mode, $m_1 + m_2$, as we can see in Fig. 1 for 283 K. This behavior is similar to that of pure CB7CB [18] and has also been reported in nonsymmetric LC dimers [21,43,44]. We have kept the same shape parameters of m_2 ($\alpha = 0.6$ and $\beta = 1$) for the fitting to Eq. (1) for $m_1 + m_2$, obtaining a very

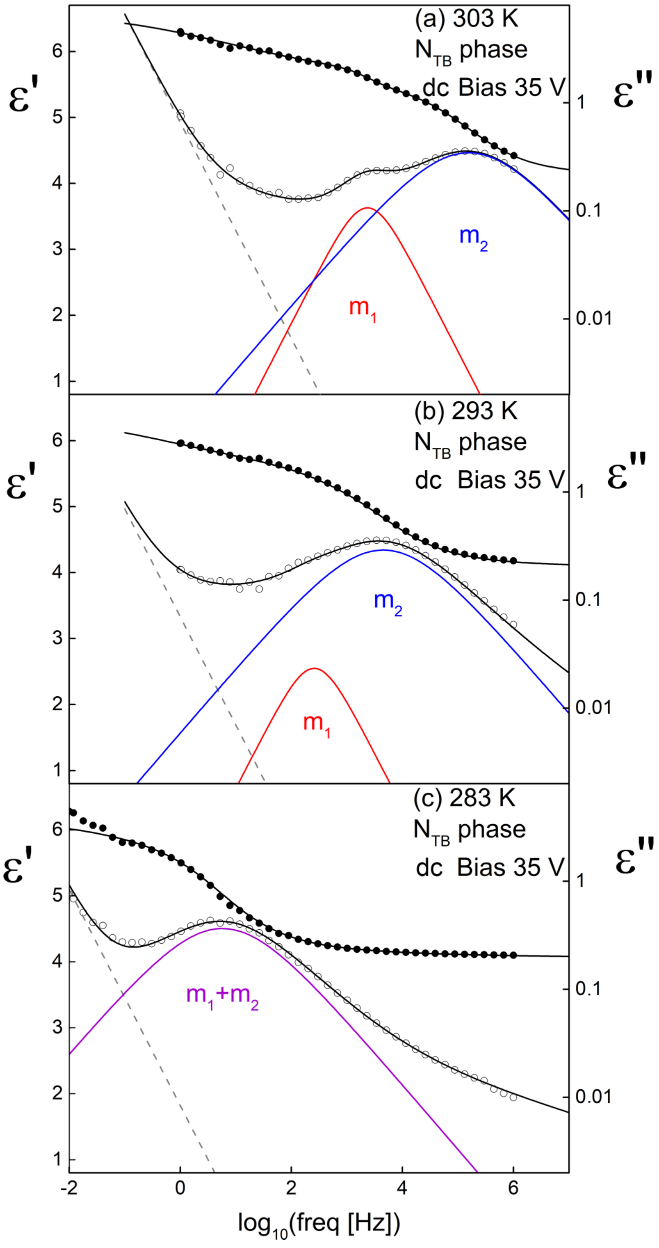

FIG. 1. Frequency (in $\log_{10}$ scale) dependence of the complex dielectric permittivity for the mixture at (a) 303 K, (b) 293 K, and (c) 283 K under a dc bias of 35 V. Filled circles account for the experimental real part, empty circles for the experimental imaginary part (in $\log_{10}$ scale); fittings to Eq. (1) are shown by the solid lines: Black solid lines show the whole dielectric response and colored solid lines represent the deconvoluted relaxation modes (just for the imaginary part of the dielectric permittivity). Gray dashed lines account for dc conductivity.

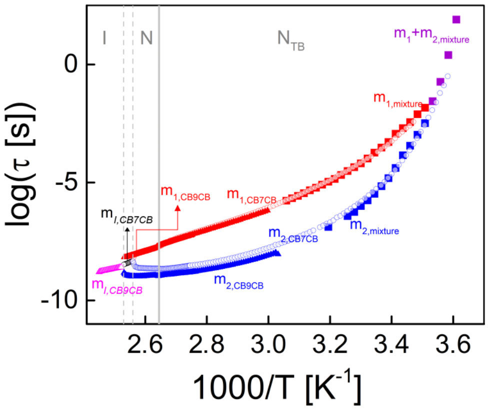

FIG. 2. Arrhenius plot of the relaxation frequencies of the different modes for the three compounds. Pink triangles account for the isotropic mode (m_I) of CB9CB, black circles for m_I of CB7CB, red and blue symbols for m_1 and m_2, respectively (triangles for CB9CB, squares for the mixture, and empty circles for CB7CB), and purple squares for the $m_1 + m_2$ mode of the mixture.

good fitting, as can be appreciated in Fig. 1. We will deepen these results in the next Sec. III B.

The behavior of the characteristic time τ of the relaxation modes with temperature is represented in the Arrhenius plot of Fig. 2. From dielectric spectroscopy measurements, we obtain a single glass transition temperature T_g at ∼276 K, as can be directly seen from experimental data. This glass transition temperature is the same, within the experimental error, as that for pure CB7CB obtained from dielectric spectroscopy [18]. We must note that a double glass transition has been detected in some nonsymmetric LC dimers [21,43,44], each of the glass transitions being due to the vitrification of one of the rigid moieties of the dimer. In the present case, the symmetric character of the dimer leads to a single T_g, as will be verified in the next section.

In the Arrhenius plot (Fig. 2) we can observe that the relaxation times of both the m_1 and m_2 modes of the mixture at low temperatures are the extrapolations of the relaxation times of the same modes for pure CB9CB. Moreover, it can be observed that, far from the glass transition, the modes of CB9CB and the mixture are faster (lower relaxation times at a same temperature) than those of CB7CB. As the linking chain is larger in CB9CB than in CB7CB, the motions of both cyanobiphenyl units in the former are less coupled (and, therefore, freer) than those of the latter, allowing faster reorientations. From these results, it looks like the small amount of CB7CB we dope pure CB9CB with to form the mixture is sufficient to avoid crystallization of a large amount of the material, but it does not seem to affect the molecular interaction properties of the dominant compound in the mixture, which is CB9CB-like. The value of T_g for pure CB9CB should be the same as that for CB7CB and the mixture, that is, ∼276 K.

As a final comment, it can be seen that the relaxation modes have super-Arrhenius behavior and, so, their activation energies are temperature dependent. We have estimated the activation energy of the $m_1 + m_2$ mode just when reaching the glass transition, calculating the slope of the curve formed by its relaxation time vs $1/T$ at T_g, obtaining $E_a(T_g)\sim10^6$ kJ/mol (∼10 eV/molecule).

Further research must be made to confirm our suppositions with respect to the CB9CB-like behavior of the relaxation modes of the mixture and the relative amount of crystallized material between the three compounds. This research is presented in the next subsection.

B. Thermally stimulated depolarization currents (TSDCs)

TSDC experiments allow us to obtain the glass transition temperature not just of CB7CB and the mixture, but also of CB9CB. CB9CB indeed crystallizes when cooling down before reaching the glass transition, but just partially, and the magnitude of the noncrystallized part of the compound is enough to measure the value of T_g through TSDC. As we have pointed out in the previous subsection, the CB9CB-like mixture crystallizes, but its crystalline fraction is smaller than that of pure CB9CB.

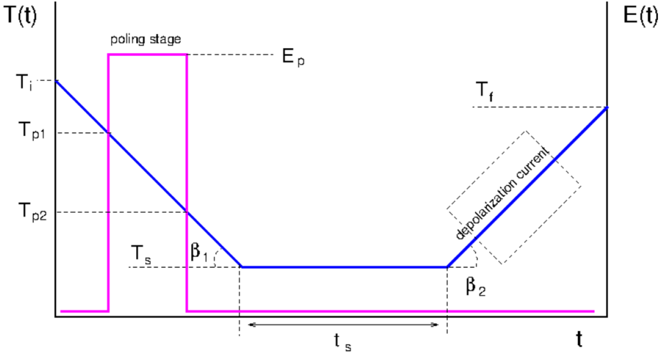

Scheme 3: Summary of TSDC experiment with NIW poling.

A relaxation mode can be described by the sum of several elementary (Debye-like) contributions. This is habitual, but not exclusive, in compounds where different mechanisms are responsible for the same relaxation mode, like dimers or polymers. The dielectric relaxation modes m_1 and m_2 of the studied LC dimers can be considered as the sum of several elementary processes, each of them with a characteristic relaxation time τ. The $m_1 + m_2$ mode close to T_g is even more complex than m_1 and m_2 separately. The separation of these distributed modes into elementary processes cannot be done directly using dielectric spectroscopy experiments. However, one of the strengths of the TSDC technique is its ability to analyze the elementary contributions of a distributed relaxation mode [21,43,60–64].

TSDC measurements start with the material in the liquid phase at 403 K. Then, the sample is cooled to 255 K at a cooling rate of 20 K/min, which is the maximum cooling rate allowed by our setup. Under these conditions, there is always some fraction of the sample that vitrifies. Nonisothermal window (NIW) poling was used in the measurements, as summarized in Scheme 3. Details of the experiments for CB9CB, CB7CB, and their binary mixture are reported in the Supplemental Material [65].

Two different typologies of poling windows were employed. On the one hand, a broad poling window (T_{p1}–$T_{p2} \sim 15$ K) was applied to each sample to obtain an overall view where as many as possible modes associated with the glass transition are activated. This measurement is roughly equivalent to a dielectric loss measurement at very low frequencies ($<10^{-3}$ Hz) [56]. With this kind of experiment, we analyze the distributed relaxation modes and, consequently, obtain the glass transition temperature of each one. On the other hand, narrow poling windows ($T_{p2} = T_{p1}$–1 K) were used to perform a relaxation map analysis (RMA). In this procedure, the poling electric field is applied just in a narrow temperature window during the cooling stage. As a consequence, only elementary modes with a single relaxation time are activated. Repeating the experiment with different T_{p1} temperatures allows us to separate global relaxation modes into their elementary contributions. Therefore, we can quantify the relative contribution (weight) of each of these modes and determine the distribution of relaxation times (DRT) of a distributed relaxation mode.

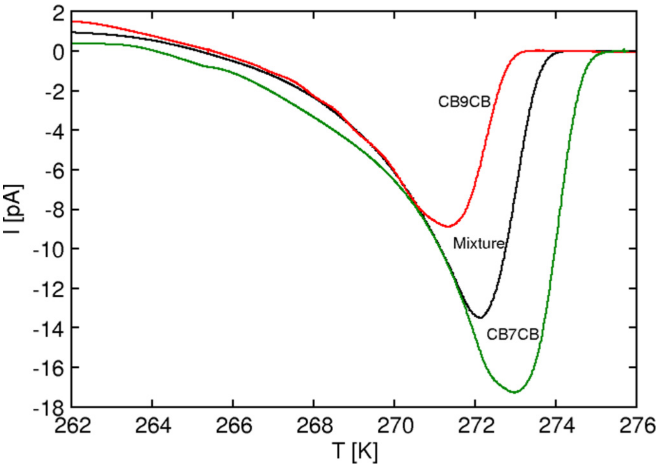

FIG. 3. Depolarization currents for broad poling window experiments.

We start the discussion with the broad window poling measurements, which give an overall picture of the relaxation. These results are plotted in Fig. 3. The maximum value of each peak is at the glass transition temperature for the corresponding compound [60]. The glass transition temperatures T_g for both pure compounds and the mixture, obtained from MDSC, dielectric spectroscopy, and TSDC, are listed in Table I.

The difference between the values of T_g obtained from different measurements comes from the fact that the glass transition is time dependent and, therefore, it is sensitive to the experimental procedure. TSDC measurements, that are able to discern between close glass transition temperatures [21,43] show that there is just one T_g for each compound and that the values of the three compounds are very close to each other (the three values are in a range of ~1.5 K), confirming the results from dielectric spectroscopy.

Figure 3 also shows that the dielectric strength or polarizability (related to the area of the current peak) is greater for CB7CB than for CB9CB, the value for the mixture being

TABLE I. Glass transition temperatures T_g of the studied compounds, obtained from MDSC, dielectric spectroscopy, and TSDC. All temperatures are in K.

	MDSC	Dielectric spectroscopy	TSDC
CB9CB	277 [33]	276[a]	271.5[a]
Mixture	277 [57]	276[a]	272.0[a]
CB7CB	277 [18]	276 [18]	273.0[a]

[a] Results obtained in the present work.

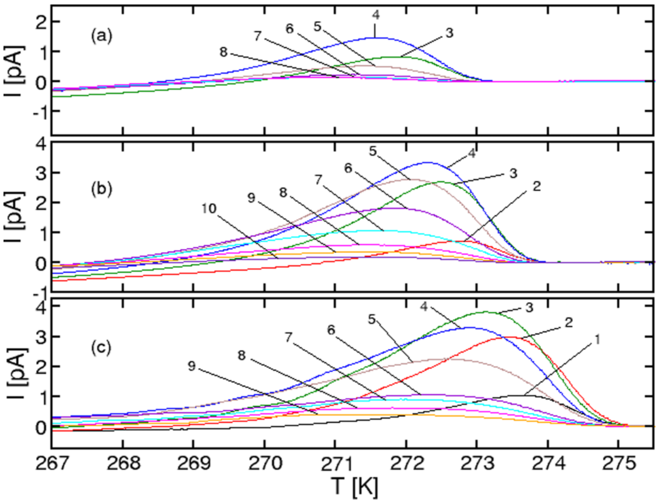

FIG. 4. Relaxation map analysis (RMA) of the three samples: CB9CB (a), the mixture (b), and CB7CB (c). The curves are numbered from (1) to (10), the number indicating the corresponding poling temperature: (1) accounts for $T_p = 275$ K, (2) for $T_p = 274$ K, (3) for $T_p = 273$ K, (4) for $T_p = 272$ K, (5) for $T_p = 271$ K, (6) for $T_p = 270$ K, (7) for $T_p = 269$ K, (8) for $T_p = 268$ K, (9) for $T_p = 267$ K, and (10) for $T_p = 266$ K.

intermediate. We can assume that the peak area mostly depends on the amount of noncrystallized material. Therefore, these results confirm that the crystalline fraction is larger for CB9CB than for CB7CB, which we had already pointed out in the previous section. This is explicit evidence that the small amount of CB7CB in the mixture is capable of drastically reducing the crystalline fraction with respect to pure CB9CB. We can also note one of the strengths of TSDC: the small part of the noncrystallized material of pure CB9CB is enough to analyze the compound at the glass transition, in contrast with MDSC or dielectric spectroscopy measurements.

To analyze the different elementary contributions of each of these peaks, we present the RMA of the three compounds in Fig. 4. We can see how the global relaxation mode of each compound is formed by several elementary relaxation modes, centered at different temperatures. The weight of a single peak, N, is proportional to its area multiplied by its poling temperature [61]. This weight is the contribution of the corresponding elementary relaxation mode to the entire mode [61]. The poling temperature for which the contribution (weight) is maximum is called the optimum poling temperature (T_{po}).

For the modeling, first-order dynamics is assumed for the depolarization current $J(T)$ of the relaxation mode:

$$J(T) = \frac{P_0}{\tau(T)}\exp\left[\frac{-1}{\beta}\int_{T_i}^{T}\frac{dT}{\tau(T)}\right], \tag{2}$$

where P_0 is the initial polarization, $\tau(T)$ is the relaxation time, T_i is the initial temperature, and β is the heating rate. A more detailed explanation of this procedure can be found elsewhere [62,63].

We have tested two different models for evaluating the relaxation time $\tau(T)$. If we assume that the relaxation time depends only on the temperature, we have the Arrhenius model,

$$\tau(T) = \tau_0\exp\left[\frac{E_a}{RT}\right], \tag{3}$$

with E_a being the activation energy.

An extension of the Arrhenius model is the Tool-Narayanaswami-Moynihan (TNM) model [66],

$$\tau(T) = \tau_0\exp\left[\frac{xE_a}{RT} + \frac{(1-x)E_a}{RT_f}\right], \tag{4}$$

where the relaxation time depends on the temperature and, also, on the memory effects of the structural conformation in the system. Such memory effects are parametrized through the fictive temperature T_f and the nonlinearity parameter x. The Arrhenius model ($x = 1$) is linear in the sense that it describes a linear relationship between $\ln(\tau)$ and $1/T$. When such a relationship is not linear, the Arrhenius model is not accurate and $x < 1$. The parameter x can be considered as a measure of the dependence of the activation energy on factors other than temperature. These factors are represented by the fictive temperature of the nonequilibrium system, which is the temperature of another system at equilibrium with the same conformation. All the fitting results are summarized in the Supplemental Material [65].

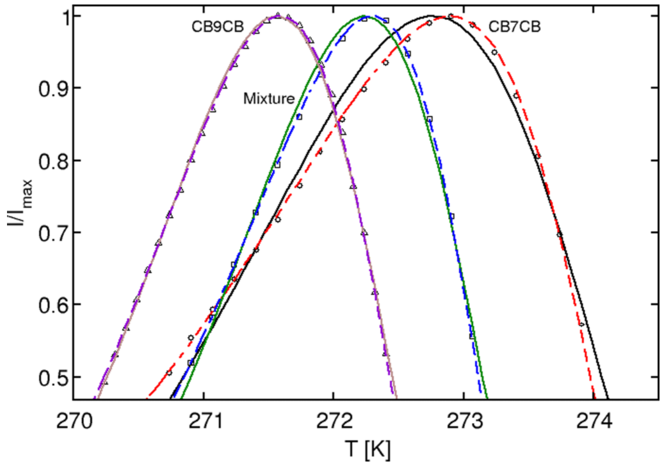

FIG. 5. Fitting results of the experimental peaks corresponding to the optimum poling temperature T_{po} of CB9CB (triangles), the mixture (squares), and CB7CB (circles), using the Arrhenius (straight lines) and TNM (dashed lines) models.

We can see from Fig. 4 that the optimum poling temperature (T_{po}) is 272 K for the three compounds (from both Arrhenius and TNM fittings). Figure 5 shows the fittings of the peaks corresponding to T_{po} for the three compounds to the Arrhenius (straight lines) and TNM (dashed lines) models. The peaks are best fitted by the TNM model in CB7CB. For CB9CB, the difference between both fittings is small. The mixture has an intermediate behavior between both pure compounds in terms of the difference in fittings. The values of the parameter x obtained from the fittings to the TNM model at T_{po} are 0.90 for CB9CB, 0.81 for the mixture, and 0.71 for CB7CB.

In glassy polymers, the nonlinearity parameter is representative of the structural state of the system. The structural state can be related to the molecular free volume. Even if for LC dimers the frozen dynamic disorders are not structural, but intramolecular [21], we can talk about the free volume. Thus, the x parameter from the TNM model is related to the free volume, which diminishes as the sample cools down. When approaching the glass transition, nonlinear effects can arise, leaving the free volume out of equilibrium. This is the case of CB7CB and, to a lesser degree, of the mixture. In CB9CB, the crystalline fraction is high, so just a small part of the material vitrifies. Spherulites are formed and an amount of vitrified material gets trapped, leading to a saturation of the free volume that translates into linear or quasilinear behavior in terms of the x parameter.

We can make a simple qualitative study of the distributed character of the relaxation modes of CB9CB, the CB9CB-like mixture, and CB7CB and also of some nonsymmetric dimers of the series α-(4-cyanobiphenyl-4′-oxy)-ω-(1-pyreniminebenzylidene-4′-oxy)alkanes (CBOnO.Py) from Refs. [21,43], with $n = 5$, 7, 9, and 11. These nonsymmetric LC dimers show three relaxation modes by dielectric spectroscopy and the two ones with higher frequencies (m_2 and $m_{1\mathrm{H}}$) converge at, or close to, the glass transition. These modes (m_2 and $m_{1\mathrm{H}}$) behave in a similar way to those of the symmetric LC dimers we have studied in the present work (m_2 and m_1). From dielectric spectroscopy measurements, it is shown that they are non-Debye when fitting the relaxation times to the Havriliak-Negami equation. Close to the glass transition, the converging modes ($m_2 + m_1$ or $m_2 + m_{1\mathrm{H}}$) are Cole-Cole (Cole-Davidson in the case of CBO11O.Py). From TSDC, they show non-Arrhenius behavior, with $x < 1$ when fitted to the TNM model.

The low-frequency mode of the nonsymmetric dimers ($m_{1\mathrm{L}}$) vitrifies at a higher T_g, compared with the other two. When fitting the dielectric spectroscopy data to the Havriliak-Negami equation they are shown to be Debye-like. Moreover, the TSDC data are well fitted to the Arrhenius model. There is an evident relationship between a Debye-like dielectric mode and an Arrhenius TSDC mode. A future interesting study would be to find a quantitative relationship between the nonlinearity parameter x and the α and β parameters of Eq. (1), but it is beyond the scope of the present work.

We can obtain further insight into the glassy behavior of the compounds, by studying the relationships between the poling temperature and the weights of the peaks, with their activation energies. Figure 6 presents the activation energy E_a obtained by TNM, in front of the poling temperature T_p. It can be noted how the activation energy increases with the poling temperature. It can also be observed how the activation energy of the mixture is similar to that of CB9CB, which is indicative of the CB9CB-like character of the mixture.

The inset of Fig. 6 presents the DRT for each compound, that is, the dependence of the weight of each elementary mode N with the activation energy, both quantities obtained by TNM. As mentioned before, these weights are obtained by multiplying the area of the RMA peaks from Fig. 4, as calculated from the fitting parameters, by the poling temperature [61]. It can be observed how the weight of the modes is lower for CB9CB than for CB7CB, with the values of the mixture being intermediate. As the amount of crystalline material highly influences polarizability, the weight of the modes is a measure of the amount of crystallized material in a compound.

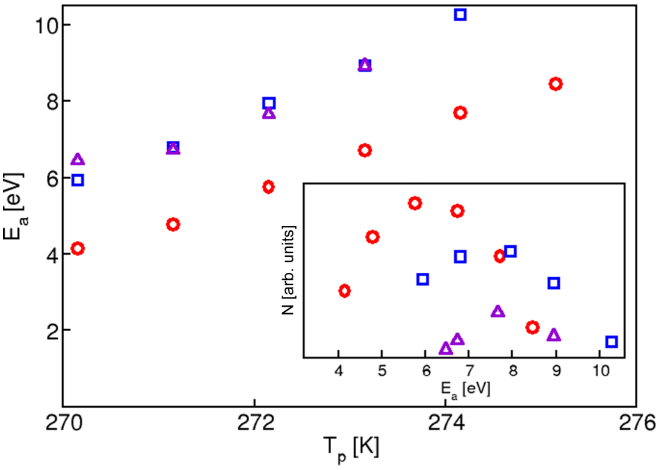

FIG. 6. Activation energy per molecule in front of the poling temperature (main graph) and distribution of relaxation times, DRT (inset), for CB9CB (triangles), the mixture (squares), and CB7CB (circles), obtained from the TNM model.

These results confirm the already discussed differences in the crystalline fraction of each of the samples.

It is important to note that the values of E_a from TSDC measurements are comparable to that estimated from dielectric spectroscopy results (∼10 eV), which shows once again the complementarity between both experimental techniques.

As a final comment, it can be seen in the Supplemental Material [65] that the TNM model gives higher values for the activation energy than the Arrhenius one. This is a characteristic feature of the TNM model, where the activation energy accounts not only for the influence of temperature, as does the Arrhenius model, but also for the nonlinearity of the mode.

IV. CONCLUDING REMARKS

We have investigated the behavior of the dielectric relaxation modes of the supercooled N_{TB} phase close to the glass transition of a CB9CB-like compound. Dielectric spectroscopy and TSDC results show that CB9CB and CB7CB form a mixture with a single glass transition temperature for small concentrations of CB7CB (the mole fraction of CB9CB being 0.96). From dielectric spectroscopy, it seems that at intermediate temperatures the relaxation modes of the mixture, measured at low temperatures, meet those of pure CB9CB, measured at high temperatures. Moreover, far from the glass transition, the molecular reorientations of pure CB7CB are slightly slower than those of CB9CB and the mixture: The flexible linking chain is shorter in CB7CB and, thus, the rigid cyanobiphenyl groups are more coupled and molecular reorientations are less free. These results seem to indicate that the mixture is CB9CB-like in terms of inter- and intramolecular interactions.

TSDC measurements are complementary to those from dielectric spectroscopy, and improve the results of the latter mainly in three aspects, for the dynamic analysis of vitrifying compounds close to the glass transition: (1) they are more accurate when discerning between one or several close glass transition temperatures; (2) they are able to analyze the elementary processes that contribute to each relaxation mode, at the glass transition; and (3) they allow the study of the glassy behavior of a compound (in the present case, CB9CB) even when just a small part vitrifies. The obtained results are comparable to those from dielectric spectroscopy with respect to the values of T_g and the (estimated) activation energy. Also, it is confirmed that a small amount of CB7CB in the mixture is able to make the material less prone to crystallization. Therefore, we can conclude that differences between the mixture and CB9CB in our results are due to the different crystalline fractions when approaching the glass transition, as is confirmed by the polarizability that can be inferred from the weight of the peaks. On the other hand, for properties that depend mainly on the interaction between molecules (or parts of molecules), such as the activation energy, the mixture is similar to CB9CB, as could be expected from its composition. This fact, advanced tentatively from dielectric results, is corroborated by TSDC measurements. Here, TSDC measurements confirm that the N_{TB} glassy state of symmetric LC dimers has just a single glass transition, due to the freezing of a single complex dielectric relaxation mode, a product of the merge of the two relaxation modes of the LC dimer.

ACKNOWLEDGMENTS

The authors are grateful to Gobierno Vasco for funding (Grant No. IT1458-22).

[1] C. T. Imrie and G. R. Luckhurst, in *Handbook of Liquid Crystals*, edited by D. Demus, J. W. Goodby, G. W. Gray, H. W. Speiss, and V. Vill (Wiley VCH, Weinheim, 1998), Vol. 2B, Chap. X, p. 801.

[2] C. T. Imrie and P. A. Henderson, Chem. Soc. Rev. **36**, 2096 (2007).

[3] D. Vorländer, Z. Phys. Chem. **126**, 449 (1927).

[4] A. C. Griffin and T. R. Britt, J. Am. Chem. Soc. **103**, 4957 (1981).

[5] A. C. Griffin and T. R. Britt, Mol. Cryst. Liq. Cryst. **92**, 149 (1983).

[6] J. W. Emsley, G. R. Luckhurst, G. N. Shilstone, and I. Sage, Mol. Cryst. Liq. Cryst. **102**, 223 (1984).

[7] J. S. Patel and S. D. Lee, J. Appl. Phys. **66**, 1879 (1989).

[8] G. S. Attard, C. T. Imrie, and F. E. Karasz, Chem. Mater. **4**, 1246 (1992).

[9] M. Stocchero, A. Ferrarini, G. J. Moro, D. A. Dunmur, and G. R. Luckhurst, J. Chem. Phys. **121**, 8079 (2004).

[10] H. J. Coles and M. N. Pivnenko, Nature (London) **436**, 997 (2005).

[11] S. M. Morris, M. J. Clarke, A. E. Blatch, and H. J. Coles, Phys. Rev. E **75**, 041701 (2007).

[12] M. Sepelj, A. Lesac, U. Baumeister, S. Diele, H. L. Nguyen, and D. W. Bruce, J. Mater. Chem. **17**, 1154 (2007).

[13] D. A. Dunmur, M. R. de la Fuente, M. A. Pérez-Jubindo, and S. Diez, Liq. Cryst. **37**, 723 (2010).

[14] M. Cestari, E. Frezza, A. Ferrarini, and G. R. Luckhurst, J. Mater. Chem. **21**, 12303 (2011).

[15] M. Cestari, S. Diez-Berart, D. A. Dunmur, A. Ferrarini, M. R. de la Fuente, D. J. B. Jackson, D. O. Lopez, G. R. Luckhurst, M. A. Perez-Jubindo, R. M. Richardson, J. Salud, B. A. Timimi, and H. Zimmermann, Phys. Rev. E **84**, 031704 (2011).

[16] J. P. F. Lagerwall and G. Scalia, Curr. Appl. Phys. **12**, 1387 (2012).

[17] K. L. Atkinson, S. M. Morris, F. Castles, M. M. Qasim, D. J. Gardiner, and H. J. Coles, Phys. Rev. E **85**, 012701 (2012).

[18] D. O. López, N. Sebastián, M. R. de la Fuente, J. C. Martínez-García, J. Salud, M. A. Pérez-Jubindo, S. Diez-Berart, D. A. Dunmur, and G. R. Luckhurst, J. Chem. Phys. **137**, 034502 (2012).

[19] V. Borshch, Y.-K. Kim, J. Xiang, M. Gao, A. Jakli, V. P. Panov, J. K. Vij, C. T. Imrie, M. G. Tamba, G. H. Mehl, and O. D. Lavrentovich, Nat. Commun. **4**, 2635 (2013).

[20] A. Hoffmann, A. G. Vanakaras, A. Kohlmeier, G. H. Mehl, and D. J. Photinos, Soft Matter **11**, 850 (2015).

[21] S. Diez-Berart, D. O. López, J. Salud, J. A. Diego, J. Sellares, B. Robles-Hernández, M. R. de la Fuente, and M. B. Ros, Materials **8**, 3334 (2015).

[22] A. Kumar, A. G. Vanakaras, and D. J. Photinos, J. Phys. Chem. B **121**, 10689 (2017).

[23] R. Walker, M. Majewska, D. Pociecha, A. Makal, J. M. D. Storey, E. Gorecka, and C. T. Imrie, ChemPhysChem **22**, 461 (2021).

[24] R. B. Meyer, in *Les Houches Summer School Theoretical Physics, Molecular Fluids* (Gordon and Breach, New York, 1976), p. 316.

[25] I. Dozov, Europhys. Lett. **56**, 247 (2001).

[26] Chadnra Shekhar Pati Tripathi, P. Losada-Pérez, C. Glorieux, A. Kohlmeier, M.-G. Tamba, G. H. Mehl, and J. Leys, Phys. Rev. E **84**, 041707 (2011).

[27] C. Meyer, G. R. Luckhurst, and I. Dozov, Phys. Rev. Lett. **111**, 067801 (2013).

[28] R. J. Mandle, E. J. Davis, S. A. Lobato, C. C. A. Voll, S. J. Cowling, and J. W. Goodby, Phys. Chem. Chem. Phys. **16**, 6907 (2014).

[29] R. J. Mandle, E. J. Davis, C. T. Archbold, S. J. Cowling, and J. W. Goodby, J. Mater. Chem. C **2**, 556 (2014).

[30] N. Sebastián, D. O. López, B. Robles-Hernández, M. R. de la Fuente, J. Salud, M. A. Pérez-Jubindo, D. A. Dunmur, G. R. Luckhurst, and D. J. B. Jackson, Phys. Chem. Chem. Phys. **16**, 21391 (2014).

[31] E. Gorecka, N. Vaupotic, A. Zep, D. Pociecha, J. Yoshioka, J. Yamamoto, and H. Takezoe, Angew. Chem., Int. Ed. **54**, 10155 (2015).

[32] C.-J. Yun, M. R. Vengatesan, J. K. Vij, and J.-K. Song, Appl. Phys. Lett. **106**, 173102 (2015).

[33] B. Robles-Hernández, N. Sebastián, M. R. de la Fuente, D. O. López, S. Diez-Berart, J. Salud, M. B. Ros, D. A. Dunmur, G. R. Luckhurst, and B. A. Timimi, Phys. Rev. E **92**, 062505 (2015).

[34] R. J. Mandle, C. T. Archbold, J. P. Sarju, J. L. Andrews, and J. W. Goodby, Sci. Rep. **6**, 1 (2016).

[35] D. A. Paterson, M. Gao, Y.-K. Kim, A. Jamali, K. L. Finley, B. Robles-Hernández, S. Diez-Berart, J. Salud, M. R. de la Fuente, B. A. Timimi, H. Zimmermann, C. Greco, A. Ferrarini, J. M. D. Storey, D. O. López, O. D. Lavrentovich, G. R. Luckhurst, and C. T. Imrie, Soft Matter **12**, 6827 (2016).

[36] D. O. López, B. Robles-Hernández, J. Salud, M. R. de la Fuente, N. Sebastián, S. Diez-Berart, X. Jaen, D. A. Dunmur, and G. R. Luckhurst, Phys. Chem. Chem. Phys. **18**, 4394 (2016).

[37] B. Robles-Hernández, N. Sebastián, J. Salud, S. Diez-Berart, D. A. Dunmur, G. R. Luckhurst, D. O. López, and M. R. de la Fuente, Phys. Rev. E **93**, 062705 (2016).

[38] D. A. Dunmur, G. R. Luckhurst, M. R. de la Fuente, S. Diez, and M. A. Pérez-Jubindo, J. Chem. Phys. **18**, 8681 (2001).

[39] S. Diez, D. A. Dunmur, M. R. de la Fuente, P. K. Karahaliou, G. Mehl, T. Meyer, M. A. Pérez-Jubindo, and D. J. Photinos, Liq. Cryst. **30**, 1021 (2003).

[40] N. Sebastián, M. R. de la Fuente, D. O. López, M. A. Pérez-Jubindo, J. Salud, and M. B. Ros, J. Phys. Chem. B **117**, 14486 (2013).

[41] N. Sebastián, N. Gimeno, J. Vergara, D. O. López, J. L. Serrano, C. L. Folcia, M. R. de la Fuente, and M. B. Ros, J. Mater. Chem. C **2**, 4027 (2014).

[42] N. Sebastián, B. Robles-Hernández, S. Diez-Berart, J. Salud, G. R. Luckhurst, D. A. Dunmur, D. O. López, and M. R. de la Fuente, Liq. Cryst. **44**, 177 (2017).

[43] J. A. Diego, J. Sellares, S. Diez-Berart, J. Salud, J. C. Cañadas, M. Mudarra, D. O. López, M. R. de la Fuente, and M. B. Ros, Liq. Cryst. **44**, 1007 (2017).

[44] D. O. López, J. Salud, M. R. de la Fuente, N. Sebastián, and S. Diez-Berart, Phys. Rev. E **97**, 012704 (2018).

[45] R. J. Mandle, Molecules **27**, 2689 (2022).

[46] P. L. Nordio, G. Rigatti, and U. Segre, Mol. Phys. **25**, 129 (1973).

[47] W. Kauzmann, Chem. Rev. **43**, 219 (1948).

[48] G. Adam and J. H. Gibbs, J. Chem. Phys. **43**, 139 (1965).

[49] J. Wong and C. A. Angell, *Glass: Structure by Spectroscopy* (Marcel Dekker, New York, 1976).

[50] A. Schönhals, F. Kremer, A. Hofmann, E. W. Fischer, and E. Schlosser, Phys. Rev. Lett. **70**, 3459 (1993).

[51] R. H. Colby, Phys. Rev. E **61**, 1783 (2000).

[52] R. Brand, P. Lunkenheimer, and A. Loidl, J. Chem. Phys. **116**, 10386 (2002).

[53] R. Puertas, M. A. Rute, J. Salud, D. O. López, S. Diez, J. K. van Miltenburg, L. C. Pardo, J. L. Tamarit, M. Barrio, M. A. Pérez-Jubindo, and M. R. de la Fuente, Phys. Rev. B **69**, 224202 (2004).

[54] R. Puertas, J. Salud, D. O. López, M. A. Rute, S. Diez, J. Ll. Tamarit, M. Barrio, M. A. Pérez-Jubindo, M. R. de la Fuente, and L. C. Pardo, Chem. Phys. Lett. **401**, 368 (2005).

[55] J. Salud, D. O. López, S. Diez-Berart, M. A. Pérez-Jubindo, M. R. de la Fuente, M. A. Rute, and R. Puertas, J. Non-Cryst. Sol. **355**, 2550 (2009).

[56] J. Van Turnhout, in *Electrets*, 3rd ed., edited by G. M. Sessler (Laplacian Press, Morgan Hill, CA, 1999), Vol. 1, Chap. 3, p. 81.

[57] B. Robles-Hernández, M. R. de la Fuente, D. O. López, N. Sebastián, J. Salud, S. Diez-Berart, and M. B. Ros, Miscibility studies on two homologue twist-bend nematic liquid crystal dimers, in *15th International Conference on Ferroelectric Liquid Crystals*, Abstracts P100 (Fyzikální ústav AV ČR, v.v.i., Prague, 2015).

[58] P. J. Barnes, A. G. Douglas, S. K. Heeks, and G. R. Luckhurst, Liq. Cryst. **13**, 603 (1993).

[59] P. Cusmin, M. R. de la Fuente, J. Salud, M. A. Pérez-Jubindo, S. Diez-Berart, and D. O. López, J. Phys. Chem. B **111**, 8974 (2007).

[60] J. Belana, P. Colomer, M. Pujal, and S. Montserrat, Macromol. Sci. Phys. B **23**, 467 (1985).

[61] A. Bernes, G. Teyssèdre, S. Mezghani, and C. Lacabanne, in *Dielectric Spectroscopy of Polymeric Materials* (American Chemical Society, Washington, DC, 1997) Chap. 8, pp. 227–258.

[62] J. A. Diego, J. Sellarès, A. Aragoneses, M. Mudarra, J. C. Cañadas, and J. Belana, J. Phys. D **40**, 1138 (2007).

[63] J. Sellarès, J. A. Diego, J. C. Cañadas, M. Mudarra, J. Belana, P. Colomer, F. Román, and Y. Calventus, J. Phys. D **45**, 505301 (2012).

[64] J. Sellarès, J. A. Diego, and J. Belana, J. Phys. D **43**, 365402 (2010).

[65] See Supplemental Material at http://link.aps.org/supplemental/10.1103/PhysRevE.106.054702 for TSDC experimental procedure and fitting details.

[66] O. S. Narayanaswamy, J. Am. Ceram. Soc. **54**, 491 (1971).